AIP | Physics of Plasmas

Effects of alpha beam on the parametric decay of a parallel propagating circularly polarized Alfven wave: Hybrid simulations

Xinliang Gao, Quanming Lu, Xin Tao, Yufei Hao, and Shui Wang

Citation: Phys. Plasmas **20**, 092106 (2013); doi: 10.1063/1.4820801
View online: http://dx.doi.org/10.1063/1.4820801
View Table of Contents: http://pop.aip.org/resource/1/PHPAEN/v20/i9
Published by the AIP Publishing LLC.

Effects of alpha beam on the parametric decay of a parallel propagating circularly polarized Alfven wave: Hybrid simulations

Xinliang Gao, Quanming Lu,[a] Xin Tao, Yufei Hao, and Shui Wang
CAS Key Laboratory of Geospace Environment, Department of Geophysics and Planetary Science, University of Science and Technology of China, Hefei 230026, China

(Received 19 June 2013; accepted 14 August 2013; published online 6 September 2013)

Alfven waves with a finite amplitude are found to be unstable to a parametric decay in low beta plasmas. In this paper, the parametric decay of a circularly polarized Alfven wave in a proton-electron-alpha plasma system is investigated with one-dimensional (1-D) hybrid simulations. In cases without alpha particles, with the increase of the wave number of the pump Alfven wave, the growth rate of the decay instability increases and the saturation amplitude of the density fluctuations slightly decreases. However, when alpha particles with a sufficiently large bulk velocity along the ambient magnetic field are included, at a definite range of the wave numbers of the pump wave, both the growth rate and the saturation amplitude of the parametric decay become much smaller and the parametric decay is heavily suppressed. At these wave numbers, the resonant condition between the alpha particles and the daughter Alfven waves is satisfied, therefore, their resonant interactions might play an important role in the suppression of the parametric decay instability. © *2013 AIP Publishing LLC*. [http://dx.doi.org/10.1063/1.4820801]

I. INTRODUCTION

Alfven waves with a finite amplitude are found to be unstable to a parametric decay in low beta plasmas.[1–11] In the process of the parametric decay, the energy of a pump Alfven wave (k_0) is gradually transferred into that of a forward ion acoustic wave (k_s) and a backward daughter Alfven wave ($k^- = k_0 - k_s$). This instability provides a possible mechanism to explain the observed decrease of the normalized cross helicity as the solar wind travelling outward.[8,12–14] The decrease of the normalized cross-helicity is considered to be caused by the sunward propagating Alfven waves, which are excited by the parametric decay.

The parametric decay of Alfven waves has also been investigated with hybrid simulations, and the effects of ion dynamics are found to play an important role even in a low-beta plasma.[11,15–20] Part of the background protons can be accelerated along the magnetic field due to Landau resonance with the forward ion acoustic waves excited during the parametric decay, forming a proton beam with the order of the local Alfven speed.[16,18,19] This may explain the observed proton velocity distributions in the fast solar wind, which typically consist of a dense core component and a beamlike component streaming away from the sun along the background magnetic field.[21–24] As a feedback, the wave-particle interactions may reduce the linear growth rate of the parametric decay, or lead to other types of instabilities.[16–18]

One important component in the fast solar wind is alpha particles, which constitute 4% of the solar wind particle number density. Alpha particles are faster and hotter than the core protons with $U_{\alpha p} \approx V_A$, and $T_\alpha \geq A_\alpha T_p$ (where T_α and T_p are the temperatures of the alpha particles and the core protons, respectively. A_α is the mass number of the alpha atom).[22,25–27] Alpha particles make a significant contribution to the total solar wind energy flux and mass flux. In the MHD frame, employing a standard linear perturbation theory, Hollweg *et al.*,[28] Gomberoff *et al.*,[29] Jayanti and Hollweg[30] found that the streaming alpha particles can modify the dispersion relation of the parametric instability, and also introduce several new instabilities at the gyroresonance of alpha particles and protons. Kauffmann and Araneda[31] studied the effects of alpha particles on the parametric decay of a circularly polarized Alfven wave propagating along the background magnetic field, and found that the increment in the thermal energy of alpha particles may lead to a reduction of the growth rate. However, in their studies, the relative drift speed between protons and alpha particles is not considered. In this paper, with a one-dimensional (1-D) hybrid simulation model, we further investigate the effects of the relative drift speed between protons and alpha particles on the parametric decay of a parallel propagating left-handed polarized Alfven wave in a proton-electron-alpha plasma system.

This paper is organized as follows. In Sec. II, the simulation model is described. The simulation results are illustrated in Sec. III. A summary and discussions are given at last.

II. SIMULATION MODEL

A 1-D hybrid simulation model with periodic boundary condition is used to study the parametric decay of a monochromatic left-handed polarized Alfven wave in a low beta plasma. In hybrid simulations, ions are treated kinetically, while electrons are described as massless fluid.[32–34] All physical quantities depend only on one spatial coordinate (x), which is parallel to the ambient magnetic field ($B_0\hat{\mathbf{x}}$).

A monochromatic left-handed polarized Alfven wave propagating along the ambient magnetic field is chosen as the pump wave, and the corresponding fluctuating magnetic field and transverse velocity are described as

[a]Author to whom correspondence should be addressed. Electronic mail: qmlu@ustc.edu.cn

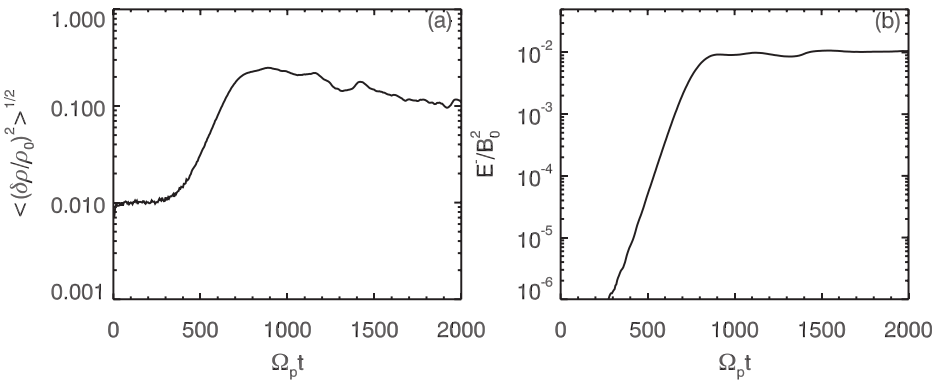

FIG. 1. Time evolution of (a) the density fluctuations $\langle(\delta\rho/\rho_0)^2\rangle^{1/2}$ and (b) the wave energy of backward propagating Alfven waves E^- with the following parameters: $k_0c/\omega_{pp} = 0.105$ and $\omega_0 = 0.099\,\Omega_p$.

$$\delta\mathbf{B}_w = \delta B[\cos(k_0x - \omega_0t)\hat{\mathbf{y}} + \sin(k_0x - \omega_0t)\hat{\mathbf{z}}]\,, \quad (1)$$

$$\delta\mathbf{u_i} = \delta u_i[\cos(k_0x - \omega_0t)\hat{\mathbf{y}} + \sin(k_0x - \omega_0t)\hat{\mathbf{z}}]\,, \quad (2)$$

where subscript i represents ion species. In our simulations, protons and alpha particles are considered, which are represented by p and α, respectively. The frequency and wave number of the pump wave are ω_0 and k_0. The dispersion relation of the pump wave is derived from the MHD equations in a cold proton-electron-alpha beam plasma[35]

$$-n_pe_p\frac{(\omega_0 - U_{p0}k_0)^2}{\omega_0 - U_{p0}k_0 - \Omega_p} - n_\alpha e_\alpha\frac{(\omega_0 - U_{\alpha0}k_0)^2}{\omega_0 - U_{\alpha0}k_0 - \Omega_\alpha} = k_0^2\,, \quad (3)$$

where n_i is the number density, Ω_i is the gyrofrequency, and U_{i0} is the bulk velocity along the ambient magnetic field.

The initial transverse velocity $\delta\mathbf{u_i}$ and fluctuating magnetic field $\delta\mathbf{B}_w$ of the pump wave satisfy the Walen's relation[17,28]

$$\delta\mathbf{u_i} = \frac{e_i}{m_i}\frac{\omega_0/k_0 - U_{i0}}{\omega_0 - U_{i0}k_0 - \Omega_i}\delta\mathbf{B_w}\,. \quad (4)$$

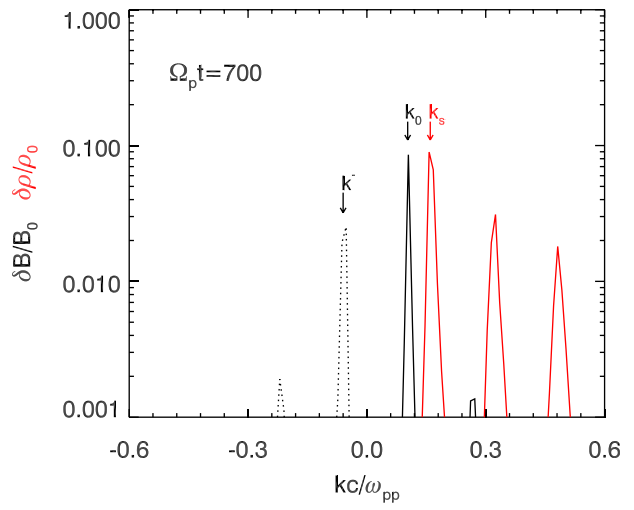

FIG. 2. The power spectra for the fluctuations of the magnetic field and density at $\Omega_p t$ =700. The parameters are same as in Fig. 1. The black lines and red lines represent the magnetic and density fluctuations, respectively. The forward modes and backward modes are denoted by the solid lines and dashed lines, respectively. The pump wave, primary ion acoustic wave, and daughter Alfven wave are marked by arrows.

In simulations described below, the velocity distribution functions of protons and alpha particles are Maxwellian, and the thermal velocity of alpha particles is the same as that of protons. The number of grid cells is $n_x = 600$, and the size of one grid cell is $\Delta x = 1.0c/\omega_{pp}$ (where c/ω_{pp} is the proton inertial length). The electron resistive length is set to be $L_r = \eta c^2/(4\pi v_A) = 0.02c/\omega_{pp}$. The time step is $\Omega_p\Delta t = 0.025$. The amplitude $\delta B/B_0$ of the pump wave is set to be 0.2. In order to save computational time, a larger amplitude of the pump wave than in reality is used in the simulations, which results in a larger growth rate of the parametric decay. The proton beta β_p is 0.01, which is similar to that in previous works.[19,20] There are on average ~900 macroparticles in every cell for each ion species. All simulations are performed in the center-of-mass frame, where the charge neutrality ($\sum_i e_i n_i = 0$, where i denotes the species of particles) and the zero current condition ($\sum_i e_i n_i U_{i0} = 0$) are satisfied initially.

III. SIMULATION RESULTS

We first describe the parametric decay of a circularly polarized Alfven wave in a proton-electron plasma system. Figure 1 displays the time evolution of (a) the density fluctuation $\langle(\delta\rho/\rho_0)^2\rangle^{1/2}$ (where ρ_0 is the initial density), and (b) the energy of the daughter Alfven waves propagating backward E^-/B_0^2. In this case, the wave number and frequency of the pump wave are $k_0c/\omega_{pp} = 0.105$ and $\omega_0 = 0.099\,\Omega_p$, respectively. We can obtain the magnetic fluctuations of the pump and daughter Alfven waves by separating the magnetic fluctuations into positive and negative helical parts with the method developed by Terasawa *et al.*[36] For a left-handed polarized pump Alfven wave, the negative helical part corresponds to forward propagating waves, whereas the positive helical part corresponds to backward propagating waves. The instability is excited at $\Omega_p t \approx 300$, and both the density fluctuation and the energy of the daughter waves begin to increase rapidly at that time. The instability saturates at $\Omega_p t \approx 700$ with the density fluctuation $\langle(\delta\rho/\rho_0)^2\rangle^{1/2} \approx 0.25$ and the energy of the daughter waves $E^-/B_0^2 \approx 0.01$.

Figure 2 shows the power spectra for the fluctuations of the magnetic field and density at $\Omega_p t$ =700. At $\Omega_p t$ =700, the parametric decay has already taken place, but the pump Alfven wave with the wave number $k_0c/\omega_{pp} \approx 0.1$ is still clearly visible. Besides the pump Alfven wave, we can also

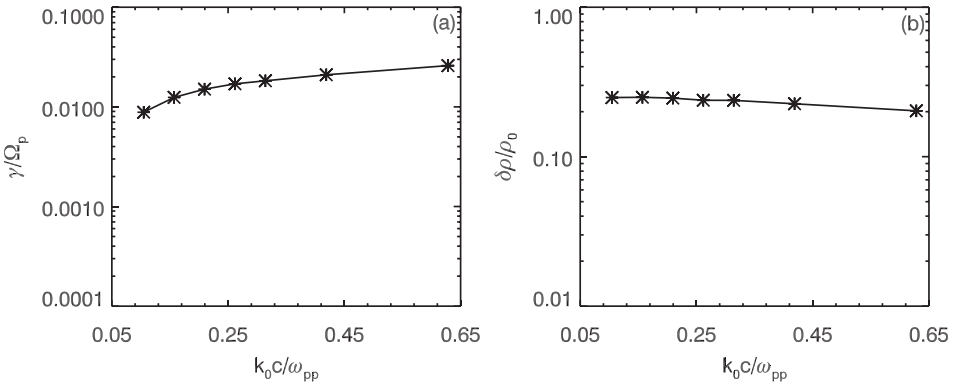

FIG. 3. The growth rates and saturation amplitude of the ion acoustic wave modes as a function of the wave number of the pump Alfven wave without alpha particles.

identify two other wave modes: the ion acoustic waves and the daughter Alfven waves propagating backward. The wave number of the ion acoustic waves with the largest amplitude is at $k_s c/\omega_{pp} \approx 0.16$, while the wave numbers of the daughter Alfven waves with the largest amplitude is $k^- c/\omega_{pp} \approx -0.06$ (black dashed lines), and they satisfy the three-wave resonant condition $k^- = k_0 - k_s$. In addition, the high-order harmonic modes of the ion acoustic waves are also excited, which then result in the generation of a weak Alfven wave propagating backward with $k^- c/\omega_{pp} \approx -0.22$.

We performed a series of simulations to demonstrate the dependence of the growth rates and saturation amplitude of the ion acoustic waves on the wave number of the pump Alfven wave, which is shown in Fig. 3. The growth rate of the parametric decay is obtained by calculating the slope of the time evolution of $\ln\langle(\delta\rho/\rho_0)^2\rangle^{1/2}$ during the linear growth phase. Consistent with previous theoretical prediction,[1,4] the growth rates of the parametric decay increase with the increase of the wave number of the pump wave. However, the saturation amplitude of the density fluctuations shows a slow decrease with the increase of k_0. The mechanism of this behavior of the saturation amplitude will be left as a future study.

Next, we consider the parametric decay of the pump Alfven wave in a proton-electron-alpha plasma system to investigate the effects of alpha particles on the parameter decay process. Here, we choose the number density of the alpha particles as $n_\alpha/n_e \approx 4\%$ (where $n_e = n_p + 2n_\alpha$ is the number density of electrons), and the relative drift speed between the alpha particles and protons ($U_{\alpha p}$) is one Alfven speed. Figure 4 displays the time evolution of (a) the density fluctuations $\langle(\delta\rho/\rho_0)^2\rangle^{1/2}$, and (b) the energy of the daughter Alfven waves propagating backward E^-/B_0^2. Here, we keep the wave number of the pump wave the same as in Fig. 1, which is $k_0 c/\omega_{pp} = 0.105$. The frequency is $\omega_0 = 0.093\,\Omega_p$, which is slightly different from that in Fig. 1 due to the existence of alpha particles. Both the density fluctuations and the energy of the daughter waves begin to increase at $\Omega_p t \approx 300$, and they saturate at $\Omega_p t \approx 700$ with the amplitude $\langle(\delta\rho/\rho_0)^2\rangle^{1/2} \approx 0.22$ and $E^-/B_0^2 \approx 0.01$. The power spectra of the fluctuations of the magnetic field and density as a function of the wave number at $\Omega_p t = 700$ are illustrated in Fig. 5. At $\Omega_p t = 700$, the wave numbers of the ion acoustic wave modes center on $k_s c/\omega_{pp} \approx 0.18$, while those of the daughter Alfven waves are around $k^- c/\omega_{pp} \approx -0.08$. We can also observe the high-order harmonic modes of the ion acoustic waves, and another weak daughter Alfven wave with $k^- c/\omega_{pp} \approx -0.26$. In this case, the evolution of the parametric decay is quite similar to that without alpha particles, which indicates the weak impact of the alpha beam on the instability when $k_0 c/\omega_{pp} = 0.015$ and $\omega_0/\Omega_p = 0.093$.

However, the situation changes when we change the wave number of the pump wave. Figure 6 shows the time evolution of (a) the density fluctuations $\langle(\delta\rho/\rho_0)^2\rangle^{1/2}$, and (b) the energy of the daughter Alfven waves E^-/B_0^2 propagating backward when the wave number and frequency of the pump wave are $k_0 c/\omega_{pp} = 0.314$ and $\omega = 0.249\,\Omega_0$, respectively. Both the density fluctuations and the energy of the daughter waves begin to grow at $\Omega_p t \approx 200$, and saturate at $\Omega_p t \approx 600$ with the amplitude $\langle(\delta\rho/\rho_0)^2\rangle^{1/2} \approx 0.02$ and

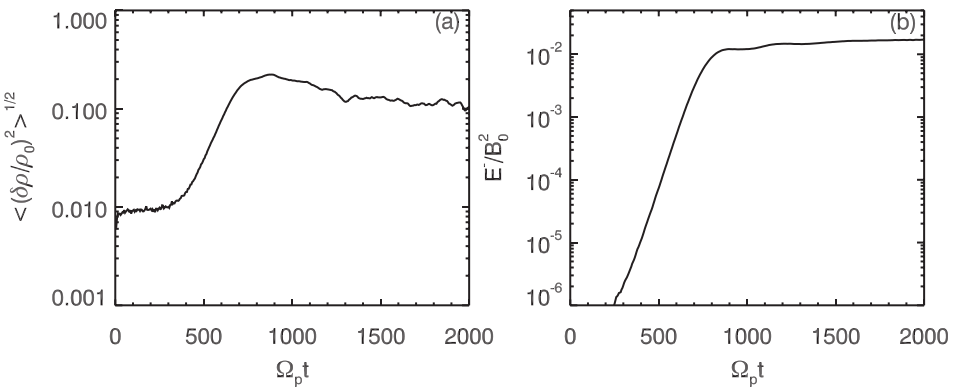

FIG. 4. Time evolution of (a) the density fluctuations $\langle(\delta\rho/\rho_0)^2\rangle^{1/2}$ and (b) the wave energy of backward propagating Alfven waves E^- with the fallowing parameters: $n_\alpha/n_e \approx 4\%$, $U_{\alpha p}/V_A = 1$, $k_0 c/\omega_{pp} = 0.105$, and $\omega_0 = 0.093\,\Omega_p$.

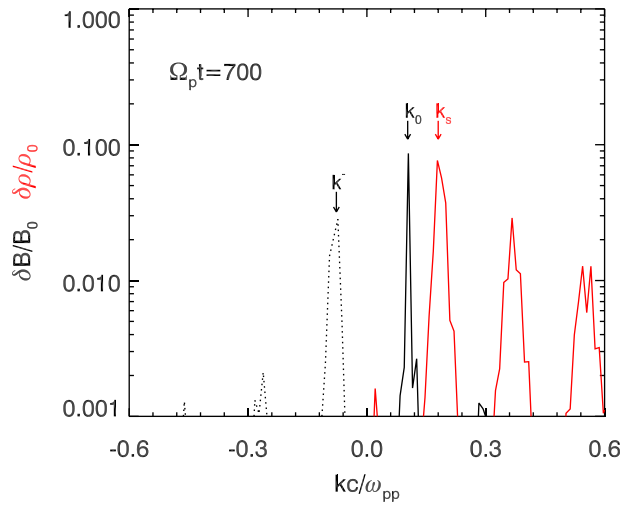

FIG. 5. The power spectra for the fluctuations of the magnetic field and density at $\Omega_p t = 700$. The parameters are same as in Fig. 4. The black lines and red lines represent the magnetic and density fluctuations, respectively. The forward modes and backward modes are denoted by the solid lines and dashed lines, respectively. The pump wave, primary ion acoustic wave, and daughter Alfven wave are marked by arrows.

$E^-/B_0^2 \approx 0.0002$. Compared with the results without alpha particles, both the growth rate and the saturation amplitude are much smaller, and the parametric decay is heavily suppressed by the alpha particles.

Figure 7 shows the growth rates and saturation amplitude of the ion acoustic wave modes as a function of the wave number of the pump Alfven wave with alpha particles. When the relative drift speed between the protons and alpha particles is one Alfven speed (black lines), we can find that the wave number of 0.26 ω_{pp}/c is just like a break point. When the wave number is smaller than 0.26 ω_{pp}/c, the growth rate increases with the increase of the wave number, and the saturation amplitude stays roughly the same. However, when the wave number is larger than 0.26 ω_{pp}/c, both the growth rate and the saturation amplitude fall rapidly until they reach the minimum values at the wave number 0.42 ω_{pp}/c. Then with the increase of the wave number, both the growth rate and the saturation amplitude recover very fast and can nearly reach the level before the break point. Compared with the results without alpha particles shown in Fig. 3, we can easily find that the alpha particles significantly suppress the parametric decay at a finite range of the pump wave k_0. However, the simulation results without the drift velocity of alpha particles (red lines) are similar to those simulations with only protons (Fig. 3). The growth rate of the parametric decay increases with the increase of the wave number, while the saturation amplitude is nearly unchanged, and there is no break point of wave number.

We conjecture that the resonant interactions between the alpha particles and the daughter Alfven waves play a key role in the parametric decay. When the alpha particles and the daughter Alfven waves satisfy the resonant condition, the parametric decay will be severely suppressed. If the alpha particles have a relative drift speed with the protons, the excited daughter Alfven waves are easy to resonantly interact with the alpha particles, then the parametric decay is suppressed at a definite range of the wave numbers. In our simulations, the drift velocity of the alpha beam is about one Alfven speed. Compared with the cases without alpha particles, the frequency of the pump wave is changed only slightly by the alpha beam, since the alpha particles are out of resonance with the pump wave. Further, with the assumption that the existence of the alpha beam having no impact on the parametric decay, the daughter Alfven waves have roughly the same wave number in both cases. Therefore, we can infer that the predicted wave number of the daughter Alfven waves is about $-0.24\ \omega_{pp}/c$ for the run with $k_0 c/\omega_{pp} = 0.42$, and its frequency is about $0.24\,\Omega_p$. In this case, the resonant condition between the alpha particles and daughter waves $\omega - \mathbf{k}\cdot\mathbf{U_{\alpha p}} = \Omega_\alpha$ is satisfied, and the parametric decay is severely quenched. Then, we can find that if alpha particles don't have a relative drift speed compared with protons, the excited daughter Alfven waves are difficult to resonantly interact with alpha particles, therefore, we cannot observe the quenching effects of alpha particles on the parametric decay.

IV. CONCLUSION AND DISCUSSIONS

By employing 1-D hybrid simulations, the parametric decay of a parallel propagating monochromatic left-handed

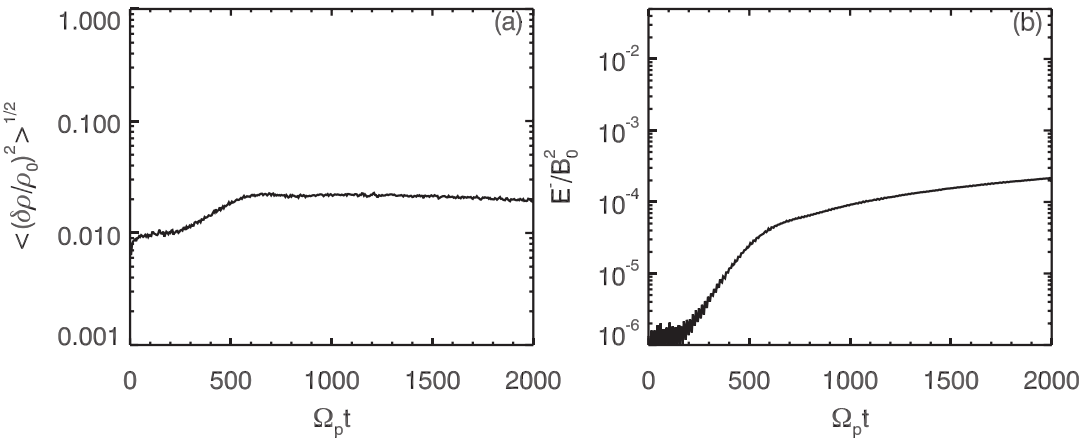

FIG. 6. Time evolution of (a) the density fluctuations $\langle(\delta\rho/\rho_0)^2\rangle^{1/2}$ and (b) the wave energy of backward propagating Alfven waves E^- with the fallowing parameters: $n_\alpha/n_e \approx 4\%$, $U_{\alpha p}/V_A = 1$, $k_0 c/\omega_{pp} = 0.314$, and $\omega = 0.249\,\Omega_0$.

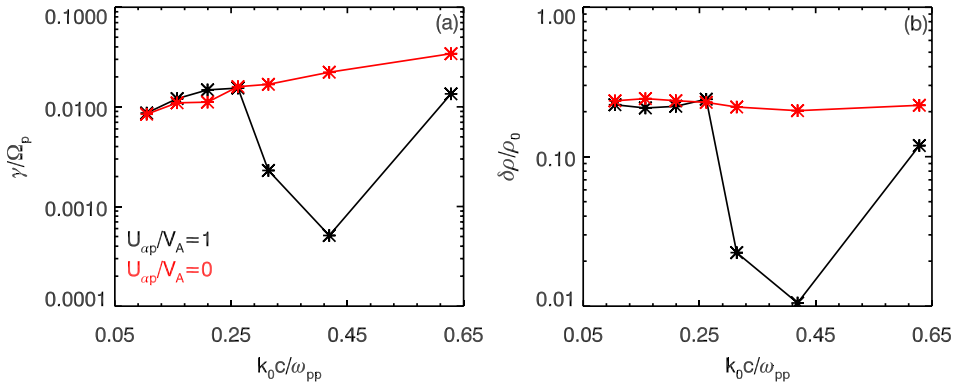

FIG. 7. The growth rates and saturation amplitude of the ion acoustic wave modes as a function of the wave number of the pump Alfven wave with alpha particles. The results for $U_{\alpha p}/V_A = 1$ and 0 are denoted by black lines and red lines, respectively.

polarized Alfven wave is investigated in a low beta plasma. When there are no alpha particles, with the increase of the wave number of the pump Alfven wave, the growth rate of the decay instability increases just as the MHD theory predicted,[1,4] while the saturation amplitude of the density fluctuations slightly decreases. After we consider the effects of the alpha particles, when there is no relative drift speed between the protons and alpha particles, the effects are ignorable. However, when there is a relative drift speed between the protons and the alpha particles, at a definite range of the wave numbers of the pump wave, both the growth rate and the saturation amplitude of the parametric decay become much smaller than the corresponding values in the cases without alpha particles, and the parametric decay is suppressed.

The *in situ* measurements of Helios and Ulysses spacecraft have showed that in the fast solar winds, the Alfvenic fluctuations are seen to evolve with the distance from the Sun: cross-helicity, which is a measure of Alfvenic correlation, decreases monotonically.[13,14] The parametric decay instability is one of the most important mechanisms to explain this phenomenon since it can locally produce the sunward propagating waves, and thus reduce the cross-helicity.[2,4,10] According to our simulation results, when there is an alpha beam with a large drift velocity, the parametric decay will be suppressed at a definite range of the wave numbers of the pump wave. Meanwhile, alpha particles are commonly observed to flow faster than the core protons by about one local Alfven speed in the typical fast solar wind.[22,23] The parametric decay of a pump Alfven wave only works in a low beta plasma, therefore, our results may be relevance of the evolution of the magnetic fluctuations in the solar wind within 0.3 AU, where the plasma beta is low.

ACKNOWLEDGMENTS

This research was supported by the 973 Program (2012CB825602 and 2013CBA01503), the National Science Foundation of China, Grant Nos. 41174124, 41274144, 41121003, and 40931053, CAS Key Research Program KZZD-EW-01, and Ministry of Education (Grant No. IRT1190).

[1]A. A. Galeev and V. N. Oraevskii, Sov. Phys. Dokl. **7**, 988 (1963).
[2]M. L. Goldstein, Astrophys. J. **219**, 700 (1978).
[3]H. K. Wong and M. L. Goldstein, J. Geophys. Res. **91**, 5617, doi:10.1029/JA091iA05p05617 (1986).
[4]V. Jayanti and J. V. Hollweg, J. Geophys. Res. **98**, 19049, doi:10.1029/93JA02208 (1993).
[5]V. Jayanti and J. V. Hollweg, J. Geophys. Res. **98**, 13247, doi:10.1029/93JA00920 (1993).
[6]J. V. Hollweg, J. Geophys. Res. **99**, 23431, doi:10.1029/94JA02185 (1994).
[7]J. A. Araneda, Phys. Scr. **T75**, 164 (1998).
[8]F. Malara, L. Primavera, and P. Valtri, Nonlinear Processes Geophys. **8**, 159 (2001).
[9]L. Gomberoff, K. Gomberoff, and A. L. Brinca, J. Geophys. Res. **106**, 18713, doi:10.1029/2000JA000384 (2001).
[10]L. D. Zanna, M. Velli, and P. Londrillo, Astron. Astrophys. **367**, 705 (2001).
[11]Y. Nariyuki and T. Hada, J. Geophys. Res. **112**, A10107, doi:10.1029/2007JA012373 (2007).
[12]B. Bavassano and R. Bruno, J. Geophys. Res. **94**, 11977, doi:10.1029/JA094iA09p11977 (1989).
[13]R. Bruno, B. Bavassano, E. Pietropaolo, V. Carbone, and H. Rosenbauer, J. Geophys. Res. **102**, 14687, doi:10.1029/97JA01083 (1997).
[14]R. Bruno, B. Bavassano, R. D'Amicis, V. Carbone, L. Sorrio-Valvo, and E. Pietropaolo, Space Sci. Rev. **122**, 321 (2006).
[15]J. A. Araneda, E. Marsch, and A. F. Vinas, J. Geophys. Res. **112**, A04104, doi:10.1029/2006JA011999 (2007).
[16]J. A. Araneda, E. Marsch, and A. F. Vinas, Phys. Rev. Lett. **100**, 125003 (2008).
[17]Y. Nariyuki, T. Hada, and K. Tsubouchi, J. Geophys. Res. **114**, A07102, doi:10.1029/2009JA014178 (2009).
[18]L. Matteini, S. Landi, M. Velli, and P. Hellinger, J. Geophys. Res. **115**, A09106, doi:10.1029/2009JA014987 (2010).
[19]L. Matteini, S. Landi, L. D. Zanna, M. Velli, and P. Hellinger, Geophys. Res. Lett. **37**, L20101, doi:10.1029/2010GL044806 (2010).
[20]Y. Nariyuki, T. Hada, and K. Tsubouchi, Phys. Plasmas **19**, 082317 (2012).
[21]W. C. Feldman, J. R. Asbridge, S. J. Bame, and M. D. Montgomery, J. Geophys. Res. **78**, 2017, doi:10.1029/JA078i013p02017 (1973).
[22]E. Marsch, K.-H. Muhlhauser, R. Schwenn, H. Rosenbauer, W. Pilipp, and F. M. Neubauer, J. Geophys. Res. **87**, 52, doi:10.1029/JA087iA01p00052 (1982).
[23]W. C. Feldman, J. T. Gosling, D. J. McComas, and J. L. Philipps, J. Geophys. Res. **98**, 5593, doi:10.1029/92JA02260 (1993).
[24]C.-Y. Tu, E. Marsch, and Z.-R. Qin, J. Geophys. Res. **109**, A05101, doi:10.1029/2004JA010391 (2004).
[25]E. Marsch, K.-H. Muhlhauser, H. Rosenbauer, R. Schwenn, and F. M. Neubauer, J. Geophys. Res. **87**, 35, doi:10.1029/JA087iA01p00035 (1982).
[26]P. A. Isenberg and J. V. Hollweg, J. Geophys. Res. **88**, 3923, doi:10.1029/JA088iA05p03923 (1983).
[27]R. von Steiger, N. A. Schwadron, L. A. Fisk, J. Geiss, G. Gloeckler, S. Hefti, B. Wilken, R. F. Wimmer-Schweingruber, and T. H. Zurbuchen, J. Geophys. Res. **105**, 27217, doi:10.1029/1999JA000358 (2000).
[28]J. V. Hollweg, R. Esser, and V. Jayanti, J. Geophys. Res. **98**, 3491, doi:10.1029/92JA02347 (1993).
[29]L. Gomberoff, F. Gratton, and G. Gnavi, J. Geophys. Res. **99**, 14717, doi:10.1029/94JA01100 (1994).

[30]V. Jayanti and J. V. Hollweg, J. Geophys. Res. **99**, 23449, doi:10.1029/94JA02370 (1994).
[31]K. Kauffmann and J. A. Araneda, Phys. Plasmas **15**, 062106 (2008).
[32]D. Winske, Space Sci. Rev. **42**, 53 (1985).
[33]K. B. Quest, J. Geophys. Res. **93**, 9649, doi:10.1029/JA093iA09p09649 (1988).
[34]D. Winske and N. Omidi, *Computer Space Plasma Physics: Simulation Techniques and Software* (Terra Sci. Publishers, Tokyo, 1993).
[35]W. Baumjohann and R. A. Treumann, *Basic Space Plasma Physics* (Imperial College Press, London, 1997).
[36]T. Terasawa, M. Hoshino, J.-I. Sakai, and T. Hada, J. Geophys. Res. **91**, 4171, doi:10.1029/JA091iA04p04171 (1986).